PRIFYSGOL
BANGOR
UNIVERSITY

Addressing knowledge gaps in the Isle of Man pollack (*Pollachius pollachius*) fishery: Collection of baseline fishery-dependant and biological data

Matthew T. Coleman, Matthew J. Garratt, Isobel S. M. Bloor, Maya Harries, Philip R. Hollyman, Felix Wagner, & Stuart R. Jenkins

Bangor University Sustainable Fisheries and Aquaculture Group
School of Ocean Sciences

Report to Isle of Man Government, Department of Environment, Food and Agriculture

Contact: i.bloor@bangor.ac.uk

August 2025

Please cite as: Coleman, M. T., Garratt, M. J., Bloor, I. S. M., Harries, M., Hollyman, P. R., Wagner, F., & Jenkins, S. R. (2025). Addressing knowledge gaps in the Isle of Man pollack (*Pollachius pollachius*) fishery: Collection of baseline fishery-dependent and biological data. Bangor University Sustainable Fisheries and Aquaculture Group, School of Ocean Sciences. 33 pages.

Table of Contents

1. Introduction

The current status of pollack (*Pollachius pollachius*) fisheries around the British Isles is one of significant political and industry concern. In 2023, ICES (International Council for the Exploration of the Sea) updated the assessment methodology for pollack from a 'category 4' data-limited approach to a 'category 2' MSY (maximum sustainable yield) approach, which revealed stocks in subareas 6–7 (comprising much of UK waters; Figure 1) to be in an overfished state (ICES, 2023). This led to a stark change in the ICES advice for the region, with zero catch recommended in 2024 and 2025 compared to a previous recommendation of ~4000 tonnes annually over the last decade. In response to this advice, the EU and UK Government have prohibited any targeted commercial fishing for pollack within subareas 6–7. The sudden closure of the fishery has resulted in a spotlight being placed on pollack stocks and the limited biological and ecological understanding of the species in UK waters, which currently hinders the development of effective recovery strategies.

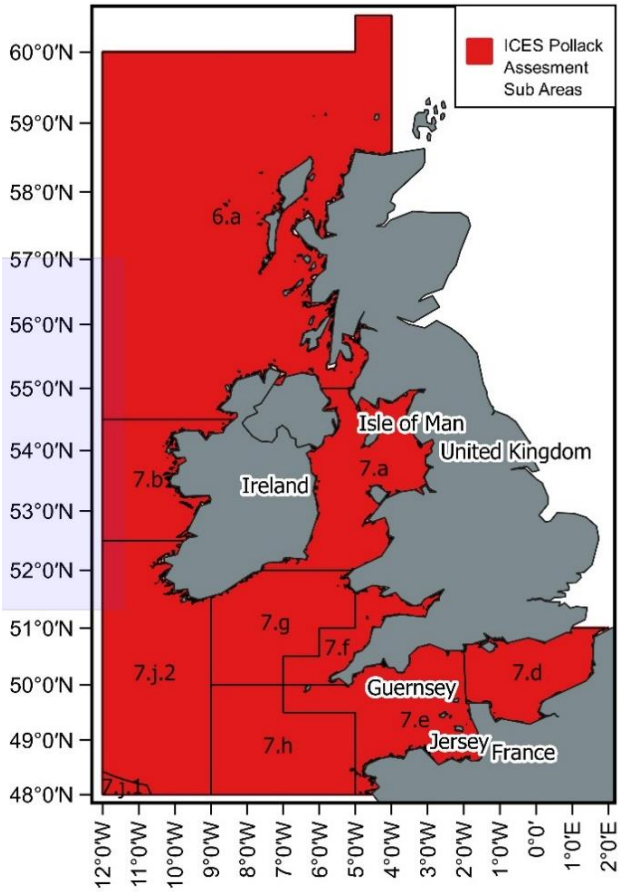

Figure 1. Map displaying the ICES subareas around the British Isles where no pollack fishing is currently permitted.

Relative to other countries in this region, the Isle of Man pollack fishery is historically small in scale, with typical landings of 2–7 tonnes year^{-1} (Figure 2), accounting for less than 0.5% of total fisheries value at first sale. It does, however, represent a microcosm of the issues facing

the pollack fisheries of larger Irish Sea nations and further afield, with no biological data currently available and no understanding of local stock health. The aim of this study, therefore, was to derive basic life history information for pollack in the Isle of Man territorial sea (including maturity, growth, and mortality) and to conduct a baseline assessment for the fishery using a suite of size-based indicators and historic landings data. In addition, stomach content analysis was carried out to explore the feeding ecology of pollack in Isle of Man waters, and genetic material collected to contribute to the wider-UK CKMR (Close-Kin Mark-Recapture) project investigating population structure and size (DEFRA, 2024).

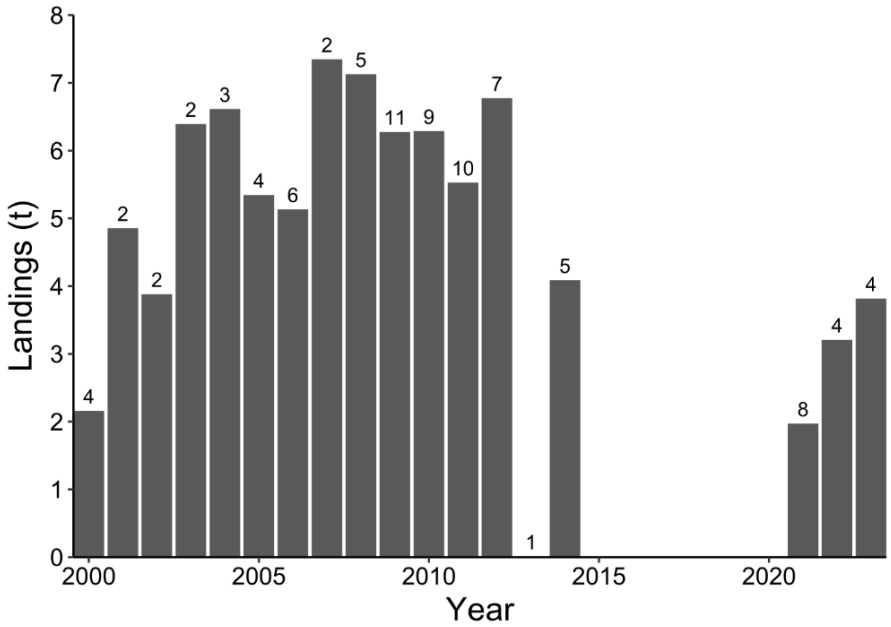

Figure 2. Total annual landings (tonnes) for the Isle of Man pollack fishery between 2000 and 2023, with numbers of active vessels displayed above the bars. No data is available from 2015 to 2020 due to differences in local catch reporting requirements during this period (see section 2.3.2 for more information).

2. Methods

2.1. Sampling methods

Data collection took place from July 2024 to April 2025, involving five commercial fishers on the Isle of Man who were active in the pollack fishery prior to its closure. Each fisher was asked to conduct regular recreational fishing trips for pollack over the duration of the study, and to either land the catch so that dissection work could be completed (biological sampling) or to measure the catch and submit the data (fisher self-sampling), depending on the time of year (Table 1). These data included the full unsorted catch from each fishing trip. Biological sampling was undertaken for the purpose of determining key life history parameters (size at maturity, size at age, mortality) and diet composition (via stomach content analysis), and occurred at two distinct time periods (summer: July–August 2024; and winter: December 2024–February 2025) to explore seasonal differences. These samples were frozen upon

receipt and subsequently processed in the laboratory (see section 2.2). Self-sampling was undertaken over the remaining months (Table 1), during which fishers recorded total body length (Figure 3) of all fish caught in order to obtain additional length-frequency data to feed into the size-based indicators. The time spent fishing (typically 4–6 hours), gear type used (handlines or trolling lines), and total catch weight (range: 16–86 kg) was also reported for each sampling trip during the study.

Table 1. Data collection timeline for the study, indicating when biological sampling and fisher self-sampling occurred along with sample sizes (n = number of fish).

Year	Month	Method	*n*
2024	July August	Biological sampling (summer)	181
	September October November	Fisher self-sampling	728
	December	Biological sampling (winter)	97
2025	January February March	Fisher self-sampling	136
	April		

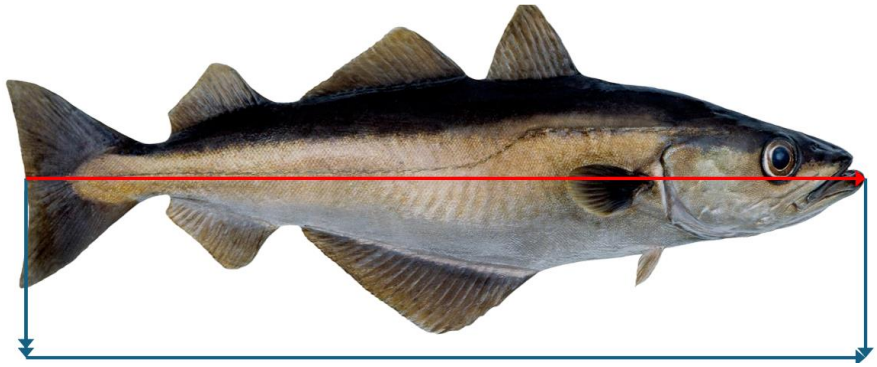

Figure 3. Diagram illustrating total body length measurement for pollack.

2.2. Laboratory methods

Fish captured during biological sampling periods (*n* = 278; Table 1) were dissected to derive information on sex, maturity, age, and diet composition. Prior to dissection, each individual was sufficiently thawed and the total length and weight of the animal recorded. In addition,

muscle tissue samples were taken from the individuals captured during summer and sent to CEFAS to provide genetic material for the CKMR project (using a genetic sampling kit provided).

2.2.1. Maturity

To determine sex and maturity status, an incision was made along the ventral side of the fish using dissection scissors, thereby exposing the internal organs and allowing the gonads (i.e. ovaries in females or testes in males) to be located (Figure 4). The gonads were then removed, weighed, and visually classified as immature or mature (Table 2). As no specific maturity staging guide currently exists for *P. pollachius*, this was done using the visual classification system developed by ICES for saithe (*P. virens*) (Bucholtz et al., 2007).

Figure 4. Photograph of incision made to expose the internal organs, with the red box indicating the location of the gonads (used for maturity assessment).

Table 2. Simplified maturity staging criteria for Pollachius spp. (more detailed sex-specific descriptions are available in Appendix Table A).

Stage	Description
1: Immature	Gonads small, thin, and translucent. Purple-reddish in colour. Located posterior in body cavity.
2: Mature	Gonads enlarged, three-dimensional, and opaque. Creamy orange/pink in colour. Fill body cavity during spawning.
3: Mature (spent/recovering)	Gonads shrunken and flabby; similar to stage 1 but more opaque. Purple-reddish in colour. Signs of previous spawning.

2.2.2. Age

To determine age, the otoliths were extracted from the head of the animal (located under the gills) using a scalpel and tweezers. Subsequently, one otolith per individual was embedded in an epoxy block, and a precision cutting machine (Struers® Secotom) was used to cut through the sagittal plane of the otolith (thus exposing the growth rings) and create two 1-mm slices for ageing. These were then secured in resin on a glass slide and imaged using an imaging microscope. Following established otolith ageing techniques, the age of each animal was estimated from the images by counting the number of annual growth rings from the core to the outer edge (Figure 5), with the core assumed to represent the hatching line. Both halves of each otolith were analysed, and all images were processed by three researchers independently (M. Garratt, M. Harries, and F. Wagner) to explore and account for any potential reader bias. The final age attributed to each animal was determined as the mode of the six otolith readings (derived from three analysts and two otolith images per individual).

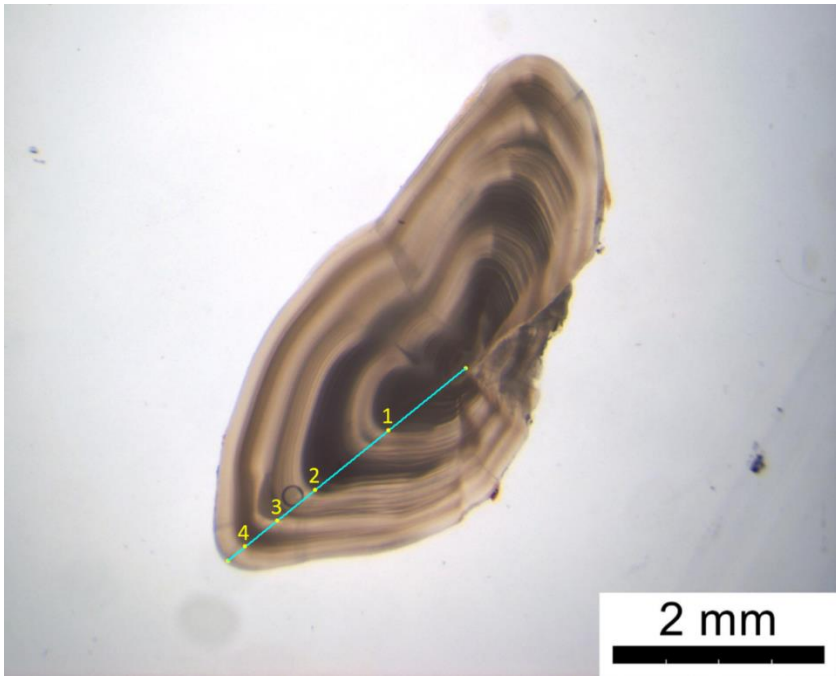

Figure 5. Example image of a pollack otolith, with the annual growth rings marked (identified as a 4-year-old individual).

2.2.3. Diet composition

Diet composition was explored in a subsample of the dissected individuals, stratified by season (summer: *n* = 62; winter: *n* = 64) and incorporating the full size distribution. Prior to analysis, the stomach of each fish was removed and preserved in a 10% formalin solution for a minimum of seven days to allow for optimal fixation of prey items. After fixation, the stomach contents were carefully extracted (including any small prey fragments), rinsed, and weighed to determine total weight, before being transferred to 70% industrial methylated spirit for subsequent storage and preservation. Stomach contents were then examined and sorted under a microscope, with prey items identified to the lowest possible taxonomic level. Recognisable prey fragments were recorded as the minimum number of individuals from which the fragments could have originated. In cases of advanced digestion, broader taxonomic categories such as Caridea and Brachyura, as well as higher-level unidentified groups like 'Unidentified Teleostei' and 'Unidentified Amphipoda', were used. Cephalopod remains typically consisted only of beaks and eyes; the presence of a complete set of beaks was interpreted as evidence of whole-animal ingestion. Similarly, teleost remains such as vertebrae and otoliths were considered valid indicators of prey consumption.

2.3. Data analysis

2.3.1. Life history parameters

Length-weight relationships for pollack were described using the equation:

$$W = aL^b$$

where W and L are total weight and total body length, respectively, and a and b are constants. To determine a and b, linear regressions were performed on natural-log-transformed length and weight, where b is the slope of the line and a is the y-intercept (converted back to the original scale as e^a). Using this method, length-weight relationships were defined for each sex and season, and all data combined.

Length at maturity was determined using logistic regressions (binomial generalised linear models with a logit link function), with total body length as a continuous explanatory variable and maturity status as a binary response variable (0 = immature; 1 = mature). The lengths at 50% maturity (L_{50}) and 95% maturity (L_{95}) were then identified from the models as the values on the x-axis at which the probability of an individual being classed as mature was 0.50 and 0.95, respectively. Confidence intervals for L_{50} and L_{95} were calculated via bootstrapping (1000 model runs).

Length at age in the population was described using the von Bertalanffy growth model:

$$L_t = L_\infty(1 - e^{-k(t-t_0)})$$

where L_t is the length at age t, L_∞ is the asymptotic length, k is the growth rate coefficient, and t_0 is the hypothetical age at which length is zero. The parameters L_∞, k, and t_0 were estimated by fitting the model to otolith length-at-age data using nonlinear regression. Initially, the full dataset (including all dissected individuals) was used; however, model convergence issues arose as the sample was heavily biased toward certain age groups (3–5 years) and lacked sufficient numbers of old individuals (> 6 years) to reliably identify L_∞. To account for this, the growth model was applied to an evenly subsampled dataset (5 individuals randomly selected per age group), and L_∞ was constrained to a biologically plausible range based on previously published values (Appendix Table B), with an added 10% buffer (55.8–108.0 cm). Median growth parameters and confidence intervals were subsequently calculated from the output of 5000 model runs (i.e. 5000 random subsamples). Due to limited sample sizes in key age groups, seasonal and sex-specific growth parameters could not be explored in this study.

To supplement the otolith analysis and evaluate the reliability of the growth parameters obtained (which are crucial for the application of size-based indicators), L_∞ and k were also estimated using ELEFAN (Electronic Length Frequency Analysis). ELEFAN identifies growth patterns by tracking modal progression in a time series of length-frequency data, and was

applied using all length measurements collected during the study (*n* = 1142), spanning a 10-month sampling period. Length data were grouped into 2 cm intervals to reduce noise and improve modal detection, with growth parameters subsequently estimated using the simulated annealing optimization algorithm. Due to highly variable sampling effort across months – particularly lower sample sizes during winter and spring compared to summer and autumn – an unseasonalised model was used.

Following the growth analysis, the instantaneous total mortality rate (Z) of the population was estimated using length-converted catch curve analysis, again based on length-frequency data grouped into 2 cm intervals. This involved plotting the natural logarithm of the number of individuals in each length class against their corresponding relative age, with Z derived by applying a linear regression to the descending limb of the curve. Estimates of the natural mortality rate (M) were then obtained using a variety of published empirical estimators for teleost fish (Then et al., 2015) (see Table 10), which also enabled the fishing mortality rate (F) to be calculated (assuming $F = Z - M$).

2.3.2. Indicators

Collection of size-frequency and life history data enabled the application of a suite of size-based indicators recommended by ICES, to explore their potential applicability for the Isle of Man pollack fishery. These indicators are intended to provide a general perception of stock status in data-limited fisheries, and highlight where growth and recruitment overfishing may be occurring (ICES, 2018). This includes assessment of: (a) the presence of large individuals in the catch (known to be indicative of fishing mortality rates); (b) the selectivity of the fishery in relation to size at maturity; and (c) the mean length of catches compared to the expected mean lengths under optimal yield and MSY scenarios (Table 3). These indicators were calculated using all length data collected during the study, combined with the estimated values for L_∞, k, L_{mat}, and M. For L_{mat}, the winter estimate was selected due to its greater reliability (see section 4.1). Confidence intervals for each biological parameter were incorporated into the assessment to evaluate uncertainty in the indicator outputs.

Table 3. Length-based indicators and corresponding reference points used by ICES (ICES, 2018). L_{mat} = length at 50% maturity; L_{opt} = optimum harvest length; M = natural mortality; L_∞, k = von Bertalanffy growth parameters.

Indicator	Calculation	Reference point	'Healthy' status	Category
$L_{max5\%}$	Mean length of largest 5%	L_∞	$L_{max5\%}/L_\infty > 0.8$	Conservation of large individuals
P_{mega}	Proportion of individuals above L_{opt} + 10%	0.3	$P_{mega} > 0.3$	
L_c	Length at 50% of modal abundance	L_{mat}	$L_c/L_{mat} > 1$	Conservation of immatures
$L_{25\%}$	25th percentile of length distribution	L_{mat}	$L_{25\%}/L_{mat} > 1$	
L_{mean}	Mean length of individuals above L_c	$L_{opt} = L_\infty \frac{3}{3 + M/k}$	$L_{mean}/L_{opt} \approx 1$	Optimal yield
L_{mean}	Mean length of individuals above L_c	$L_{F=M} = \frac{kL_\infty + 2ML_c}{2M + k}$	$L_{mean}/L_{F=M} > 1$	MSY

In addition to size-based indicators, historic commercial LPUE (landings per unit effort) data was utilised as a potential indicator of abundance. For the Isle of Man pollack fishery, this data is available for the under-10 m fleet from monthly catch returns spanning 2000 to 2014, and from the MMO's 'Record Your Catch' application for the period 2021 to 2023. Between 2014 and 2021, MSALs (Monthly Shellfish Activity Logs) were the primary reporting mechanism for under-10 m vessels in the Isle of Man, excluding demersal and pelagic species. Consequently, pollack landings data is unavailable for this period; however, the remaining time series is useful for exploring temporal trends.

For this analysis, fishing time (hours) was used as a relative measure of fishing effort due to the lack of reliable gear-specific information (e.g. number of hooks, number of lines) across the time series. For the period 2000 to 2014, fishing times were directly reported for each trip. However, for 2021 to 2023, fishing times were unavailable and vessel-specific averages derived from the 2000–2014 dataset were applied. A GAM (generalised additive model) was then used to explore how LPUE (kg hour^{-1}) varied annually across the time series, accounting for seasonal and vessel effects:

$$LPUE \sim s(Year) + Month + Vessel$$

The smoothing parameter for the year effect was estimated using REML (restricted maximum likelihood).

2.3.3. Diet composition

Diet composition was explored using a combination of multivariate statistics and univariate prey indices. PERMANOVA (Permutational Multivariate Analysis of Variance) was used to test for differences in prey community composition between seasons (summer vs. winter), sexes (female vs. male), and the interaction of season and sex. To examine potential ontogenetic diet shifts, four length classes were defined based on the size-frequency distribution of the sample (Small: 32–40 cm; s-Medium: 40–49 cm; l-Medium: 49–58 cm; Large: 58–66 cm), and a second PERMANOVA performed to test for differences in diet composition across length classes and the interaction between season and length class. Prior to these analyses, prey abundance data were square-root transformed to reduce the influence of highly abundant taxa, and a Bray-Curtis dissimilarity matrix was constructed from the transformed data to quantify differences in prey composition between stomach samples.

Two univariate indices were used to explore the prevalence of individual prey taxa: (a) relative abundance, calculated as the percentage of total prey abundance attributed to a particular taxonomic group, and (b) frequency of occurrence, calculated as the percentage of stomachs in which a particular prey item was found. These indices were subsequently used to identify the dominant prey groups characterising each season and length class.

3. Results

3.1. Size-frequency distribution

The size-frequency distribution of pollack fished during the study ranged from 12 to 75 cm (total body length), with a total of 1142 individuals caught across 34 fishing trips (range: 10–78 individuals $trip^{-1}$). The majority of the catch was above the current MCRS (minimum conservation reference size) of 30 cm, with modal abundance occurring at 40–50 cm (Figure 6). This was similar across all five fishers involved in the study (Table 4).

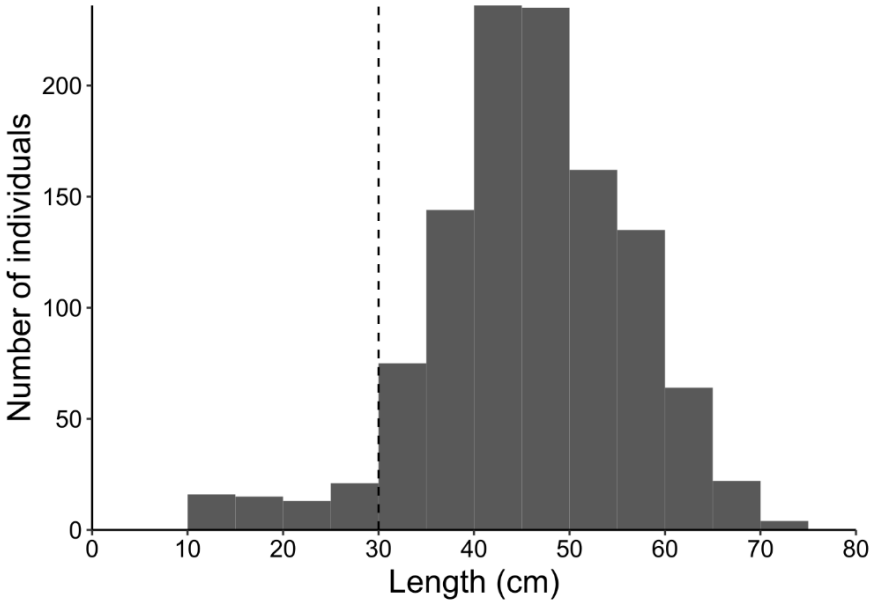

Figure 6. Size-frequency distribution (total body length) of pollack fished during the study (n = 1142). The vertical dashed line indicates the current MCRS of 30 cm.

Table 4. Median and range of sizes (total body length) fished by each participant during the study, and the proportions of catch above MCRS (30 cm).

Fisher	Median and range (cm)	≥ MCRS (%)
1	50 (31–75)	100
2	44 (20–70)	89
3	42 (12–71)	89
4	42 (24–63)	94
5	45 (22–65)	89

3.2. Life history parameters

3.2.1. Length-weight relationship

Length-weight relationships for pollack obtained during biological sampling (n = 278) are displayed in Figure 7 and Table 5. Overall, the population exhibited isometric growth ($b \approx 3$), with slightly higher growth coefficients during winter compared to summer. Minimal differences were found between females and males in both seasons.

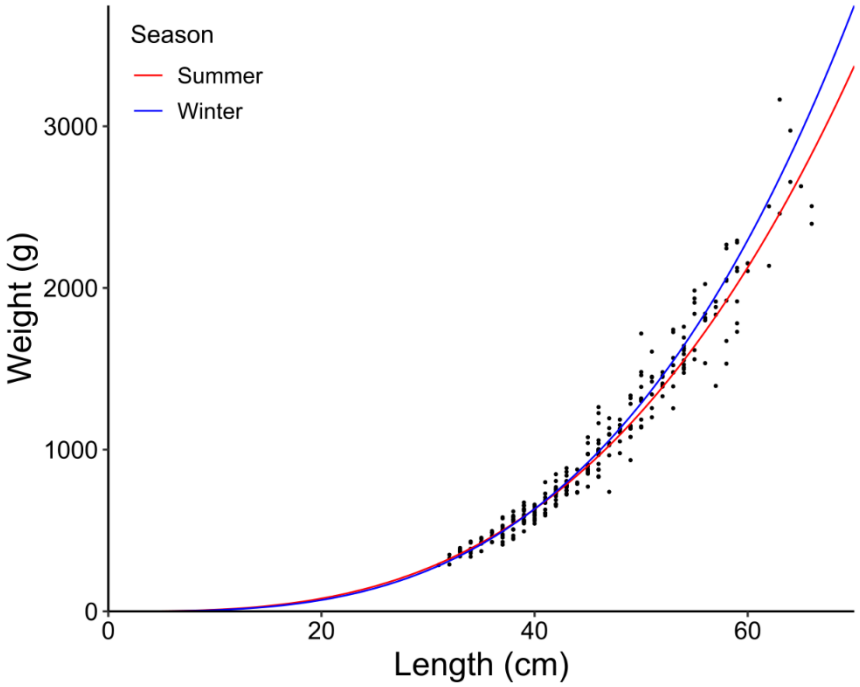

Figure 7. Length-weight relationships for pollack caught during summer (n = 181) and winter (n = 97).

Table 5. Length-weight parameters (y-intercept [a] and growth coefficient [b]) for pollack by sex and season, and all samples combined.

Season	Sex	*n*	Parameter	
			a	b
Summer	Female	92	0.009	3.011
	Male	89	0.011	2.982
Winter	Female	53	0.004	3.214
	Male	44	0.006	3.127
All	Combined	278	0.008	3.053

3.2.2. Length at maturity

Maturity assessments differed notably between seasons. During summer, pollack samples were characterised by immature (75%) and spent/recovering (25%) gonad stages, with few individuals below 50 cm classified as mature. In contrast, during winter, more than half (56%) of individuals were classified as mature and these extended to smaller sizes (Figure 8). Resulting length at 50% maturity (L_{50}) estimates were 52.1 cm (95% CI: 50.7, 53.6) in summer and 43.8 cm (95% CI: 42.1, 45.4) in winter (Figure 9; Table 6). No consistent pattern was found in sex-specific L_{50} estimates, with a higher value for males in the summer and a higher value for females in the winter.

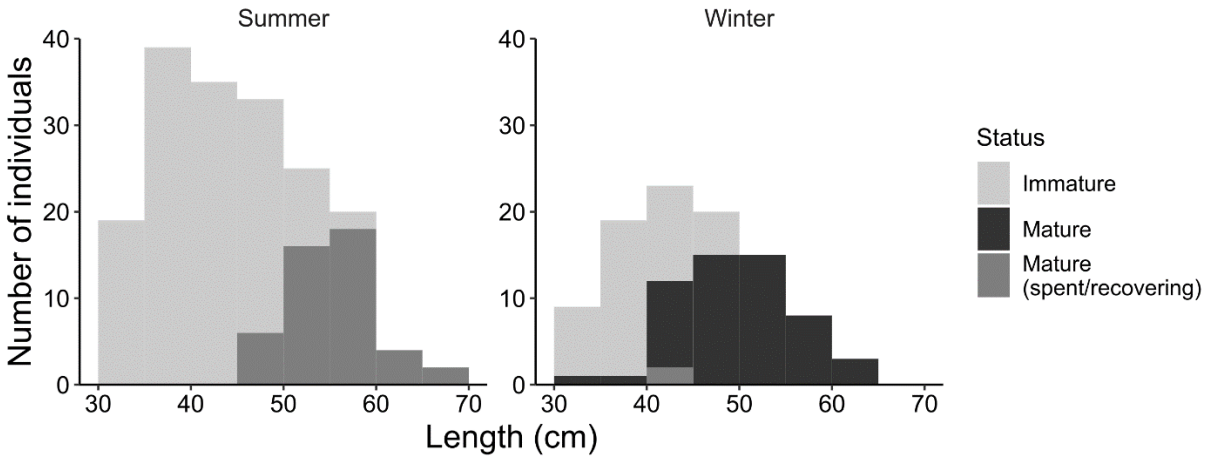

Figure 8. Size-frequency distribution of dissected pollack in summer (n = 181) and winter (n = 97), coloured by maturity status.

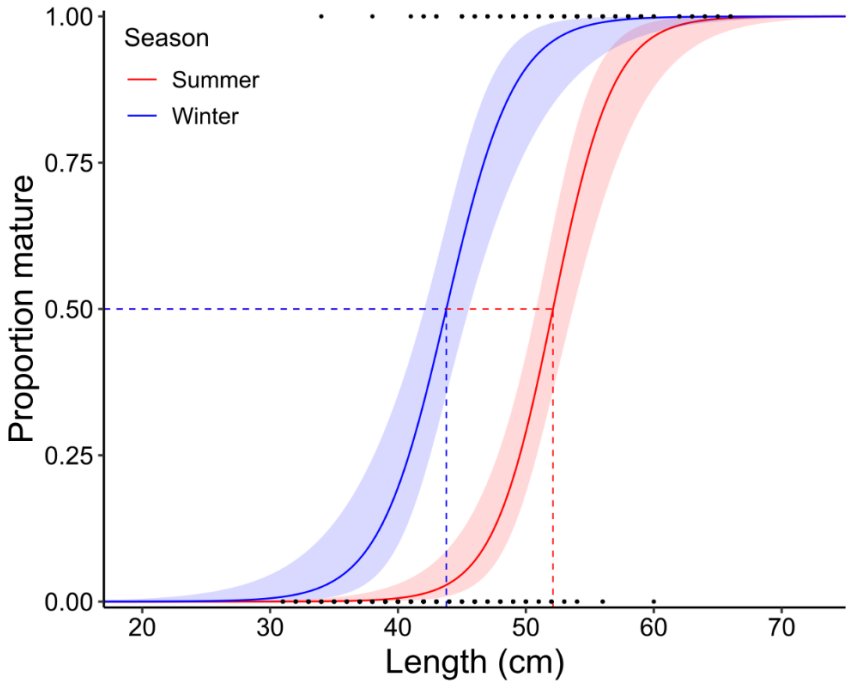

Figure 9. Maturity ogives for pollack caught during summer (n = 181) and winter (n = 97), with 95% confidence bands. Dashed lines indicate lengths at 50% maturity.

Table 6. Length at 50% maturity (L_{50}) and length at 95% maturity (L_{95}) estimates for pollack by sex and season.

Season	Sex	*n*	Parameter	
			L_{50} (95% CI)	L_{95} (95% CI)
Summer	Female	92	50.1 (48.1, 52.3)	54.8 (49.5, 58.7)
	Male	89	53.7 (51.4, 56.6)	62.4 (56.9, 68.7)
	Combined	181	52.1 (50.7, 53.6)	59.1 (56.0, 62.2)
Winter	Female	53	45.5 (43.3, 47.6)	52.5 (47.4, 56.5)
	Male	44	41.6 (38.6, 44.0)	49.6 (42.3, 55.3)
	Combined	97	43.8 (42.1, 45.4)	51.6 (48.1, 54.9)

3.2.3. Length at age

The estimated ages of fish based on individual otolith readings ranged from 2 to 10 years, with generally strong agreement across the three independent analysts (Table 7; Figure 10). Percent agreement between pairs of readers ranged from 71% to 80% and discrepancies in ages of larger than one year were rarely recorded (1% occurrence). Additionally, Bowker's tests of symmetry detected no systematic biases between any of the readers (Reader 1 vs 2: $X^2(11) = 13.06$, p = 0.16; Reader 1 vs 3: $X^2(12) = 14.39$, p = 0.28; Reader 2 vs 3: $X^2(13) = 20.19$, p = 0.09).

Table 7. Comparison of otolith age readings between pairs of analysts and average coefficients of variation (ACVs), with ACV < 10 considered acceptable for most fish species.

Reader comparison	ACV	Age difference (years)					
		-2	-1	0	1	2	3
1 vs 2	3.5	2	38	415	64	3	0
1 vs 3	4.8	3	74	372	70	2	1
2 vs 3	5.0	7	84	368	61	0	2

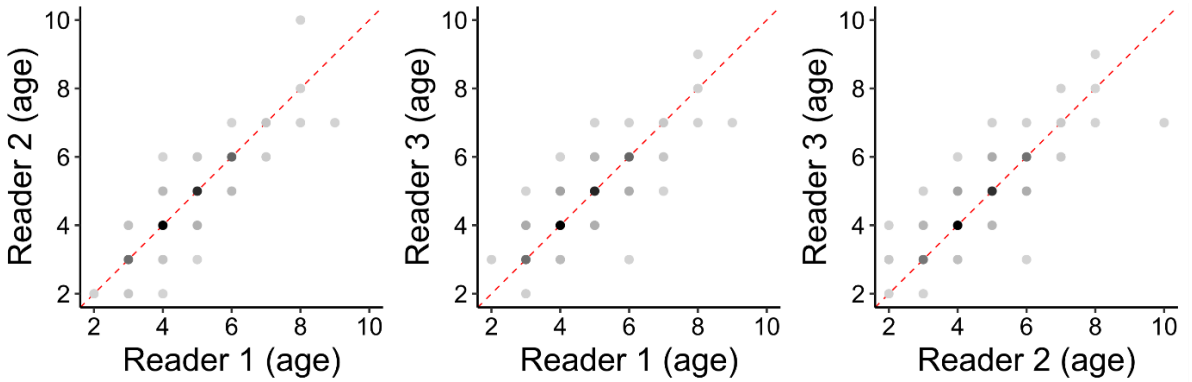

Figure 10. Scatterplots showing the relationship between otolith ages from different readers, where darker points indicate higher prevalence and dashed red lines indicate exact agreement (i.e. 1:1 relationship between ages).

The final age distribution ranged from 2 to 8 years, with the majority (87%) of individuals between 3 and 5 years of age (Table 8). Growth models run on subsampled data produced variable outputs, particularly for the asymptotic length (L_∞), which exhibited a potential range of 62–107 cm (Figure 11). Median values were 89.0 cm for L_∞, 0.13 for k (growth rate coefficient), and -1.49 for t_0 (theoretical age at length 0). In comparison, length-frequency analysis (ELEFAN) produced estimates of 91.4 cm and 0.11 for L_∞ and k, respectively (Table 9).

Table 8. Age distribution identified from otolith analysis and the median and range of sizes in each age group.

Age	*n*	Median and range (cm)
2	5	32 (31–37)
3	63	38 (31–53)
4	100	43 (33–58)
5	69	50 (33–63)
6	25	58 (46–66)
7	4	60 (46–62)
8	2	65 (64–66)

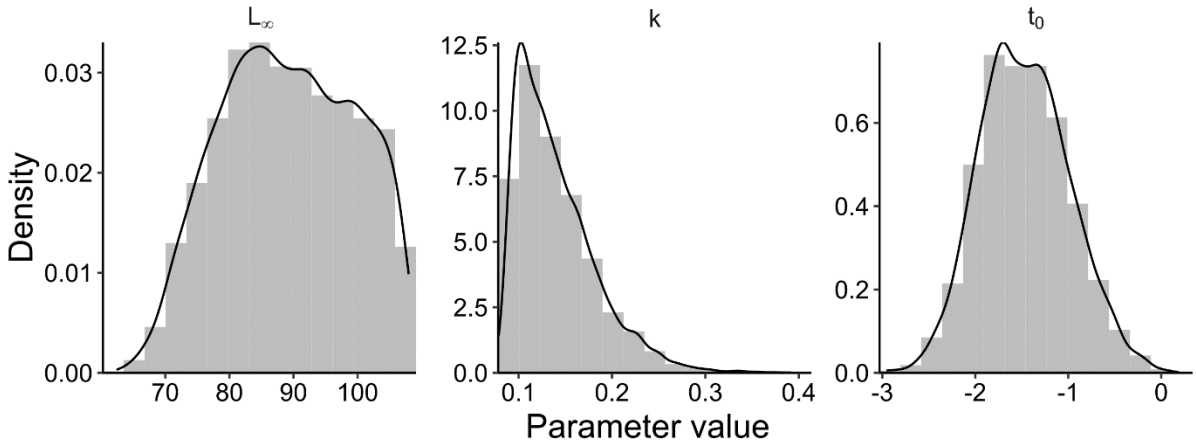

Figure 11. Distribution of parameter values obtained from von Bertalanffy growth models applied to subsampled otolith length-at-age data (5 random individuals per age group and 5000 model runs).

Table 9. Estimates for von Bertalanffy growth parameters obtained from otolith length-at-age data and Electronic Length Frequency Analysis (ELEFAN).

Method	Parameter		
	L_∞ (95% CI)	k (95% CI)	t_0 (95% CI)
Otoliths	89.0 (70.6, 106.6)	0.13 (0.09, 0.25)	-1.49 (-2.35, -0.49)
ELEFAN	91.4 (72.8, 103.7)	0.11 (0.07, 0.24)	NA

3.2.4. Mortality

The instantaneous total mortality rate (Z) for the population was estimated as 0.52 year^{-1} (95% CI: 0.44, 0.59) based on catch curve analysis, with relative ages ranging from 1 to 13 years (Figure 12). Empirical estimators indicated the natural mortality rate (M) was likely to be between 0.20 and 0.41 year^{-1} (mean: 0.31), with possible fishing mortality rates (F) between 0.11 and 0.32 year^{-1} (mean: 0.21) (Table 10).

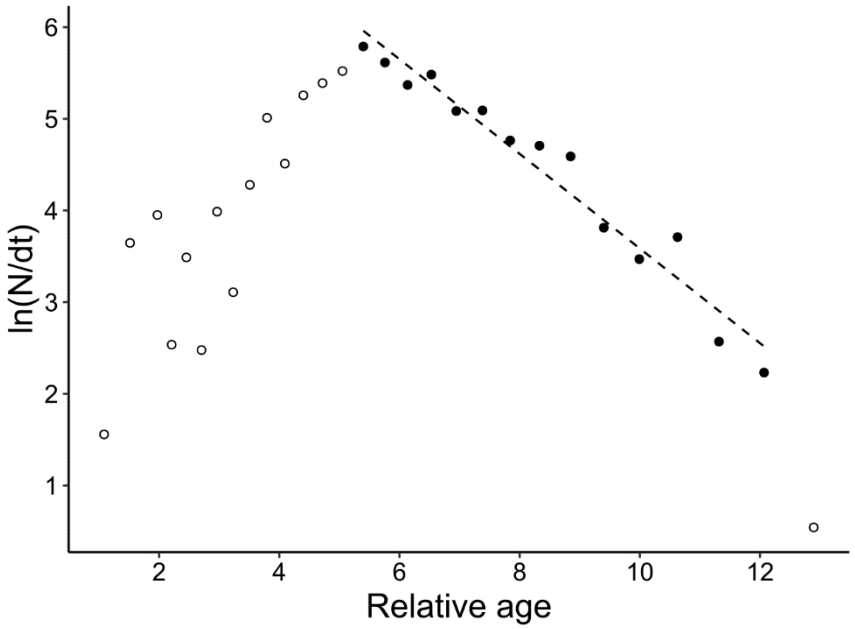

Figure 12. Length-converted catch curve of relative age and abundance (log-transformed), with the dashed line indicating the linear regression used to estimate total mortality (Z).

Table 10. Estimated values for the natural mortality rate (M) using published empirical relationships (Then et al., 2015), and corresponding fishing mortality rates ($F = Z - M$). Maximum age (t_{max}) for pollack was assumed to be 15 years (widely reported in the literature) rather than the maximum observed age in the otolith sample (8 years).

Method	**Assumption**	M	F
t_{max} empirical	$M = 5.109/t_{max}$	0.34	0.18
Hoenig (revised)	$M = 4.899t_{max}^{-0.916}$	0.41	0.11
k empirical	$M = 0.098 + 1.55k$	0.28	0.24
Pauly (revised)	$M = 4.118k^{0.73}L_{\infty}^{-0.33}$	0.20	0.32
Alverson-Carney (revised)	$M = 3k/(e^{0.41kt_{max}} - 1)$	0.33	0.19

3.3. Indicators

3.3.1. Size-based indicators

Results of the size-based indicators assessment were mixed, with a combination of negative and positive outcomes (Table 11). Firstly, indicators related to the conservation of large individuals ($L_{max5\%}$ and P_{mega}) had very wide confidence intervals, and therefore could potentially be considered as either positive or negative. It is likely, however, that both $L_{max5\%}$ (66.3 cm) and P_{mega} (0.25) are below the specified thresholds to be considered 'healthy'. In contrast, indicators for the conservation of immatures were more definitive. Both L_c (36.8 cm) and $L_{25\%}$ (41.0 cm) were smaller than the winter estimate of length at 50% maturity (43.8 cm), again suggesting 'poor' status for this aspect of the stock. On the other hand, the fishery performance indicators (proxies for optimal yield and MSY) were generally positive. Specifically, L_{mean} (49.3 cm) was similar to the estimated value for L_{opt} (48.5 cm) and exceeded $L_{F=M}$ (45.5 cm), suggesting the fishery is operating near optimal size-based yield targets.

Table 11. Results for the six length-based indicators used in the assessment, including indicator values and 'best guess' estimates for the biological reference points. Green and red boxes highlight results associated with 'healthy' and 'poor' stock status, respectively, and those marked with an asterisk (*) have particularly high uncertainty due to wide confidence intervals.

Indicator	Value	Reference point	'Healthy' status	Result (95% CI)	Category
$L_{max5\%}$	66.3 cm	$L_\infty = 90.2$ cm	$L_{max5\%}/L_\infty > 0.8$	0.74* (0.63, 0.92)	Conservation of large individuals
P_{mega}	0.25	0.3	$P_{mega} > 0.3$	0.25* (0.06, 0.59)	
L_c	36.8 cm	$L_{mat} = 43.8$ cm	$L_c/L_{mat} > 1$	0.84 (0.81, 0.88)	Conservation of immatures
$L_{25\%}$	41.0 cm	$L_{mat} = 43.8$ cm	$L_{25\%}/L_{mat} > 1$	0.94 (0.90, 0.97)	
L_{mean}	49.3 cm	$L_{opt} = 48.5$ cm	$L_{mean}/L_{opt} \approx 1$	1.02 (0.87, 1.22)	Optimal yield
L_{mean}	49.3 cm	$L_{F=M} = 45.5$ cm	$L_{mean}/L_{F=M} > 1$	1.08 (1.02, 1.14)	MSY

3.3.2. Abundance indicator

LPUE in the commercial pollack fishery ranged from 0.1 to 35.0 kg hour^{-1} between 2000 and 2014, and from 0.4 to 20.0 kg hour^{-1} between 2021 and 2023 (based on an estimated average

time fished per trip). During this period, mean annual LPUE (standardised for seasonal and vessel effects) remained relatively stable, fluctuating between 4 and 8 kg hour^{-1} (Figure 13). Fishing month ($F_{(11)} = 4.02$, $p < 0.001$) and vessel ($F_{(12)} = 43.31$, $p < 0.001$) were both identified as significant factors within the model.

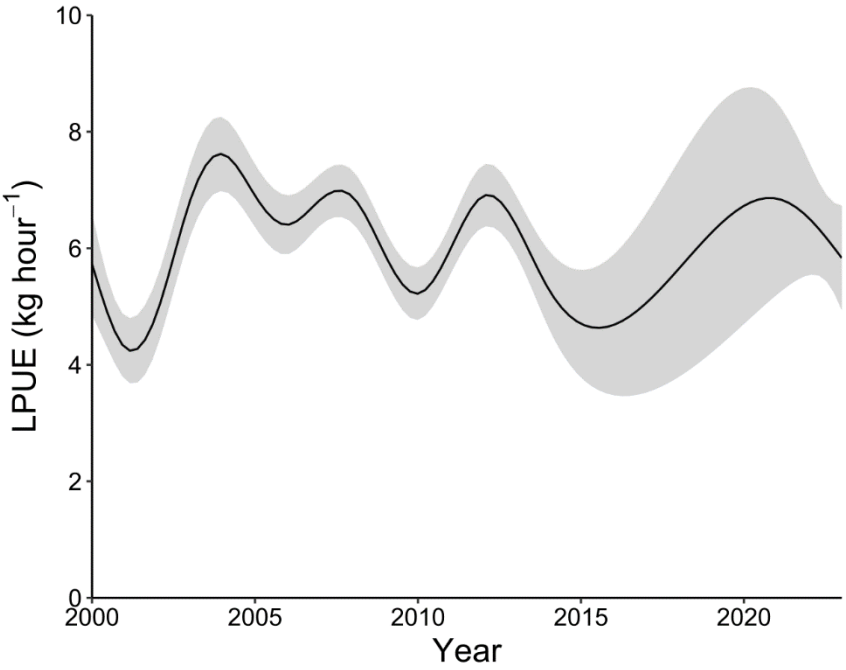

Figure 13. Standardised annual LPUE trend in the Isle of Man pollack fishery from 2000 to 2023, obtained using a GAM with the formula: LPUE ~ s(Year) + Month + Vessel. No data was available from 2015 to 2020, resulting in wider confidence intervals during this period.

3.4. Diet composition

Of the 126 individuals analysed for diet composition, only six were found with empty stomachs, with a higher prevalence during winter (~8% occurrence) compared to summer (~1% occurrence). In the remainder of the sample, prey items from over 40 distinct taxonomic families were recorded, comprising a range of crustaceans (including decapods, amphipods, and isopods), polychaetes, cephalopods, and teleost fish. Overall, the most abundant taxonomic groups were Decapoda, Polychaeta, and Amphipoda, which collectively accounted for 91% and 76% of prey items identified during summer and winter, respectively (Table 12).

Table 12. Relative abundance of major taxonomic groups identified during stomach content analysis in summer and winter (expressed as a percentage of the total number of prey items in each season). Unidentified crustacean eyes were grouped under Decapoda.

Taxonomic group	**Relative abundance (%)**	
	Summer	Winter
Decapoda	70	19
Polychaeta	<1	52
Amphipoda	21	5
Teleostei	3	7
Cephalopoda	<1	5
Isopoda	2	2
Mysida	<1	4
Other	3	6

Prey community composition differed significantly between the summer and winter sampling periods (PERMANOVA: pseudo-F = 16.35, $p < 0.001$). Summer stomach content samples were predominantly characterised by crustaceans (including large numbers of crustacean eyes and megalopa larvae), while winter samples were characterised by polychaetes (mainly *Nereididae* spp.) and cephalopods. During summer, the diet encompassed a variety of decapods such as squat lobsters (*Galatheidae* spp.), crabs (Brachyura spp., *Portunidae* spp.), and shrimp (Caridea spp.), along with frequent occurrences of teleosts, amphipods, and isopods. During winter, the dominant prey group was *Nereididae*, with other polychaete families present in small numbers, followed by cephalopods, teleosts, and crustaceans (Figure 14). No significant sex-specific differences in diet composition were identified (PERMANOVA: pseudo-F = 0.88, $p = 0.61$), and no significant interaction between season and sex was observed (PERMANOVA: pseudo-F = 0.40, $p = 0.96$).

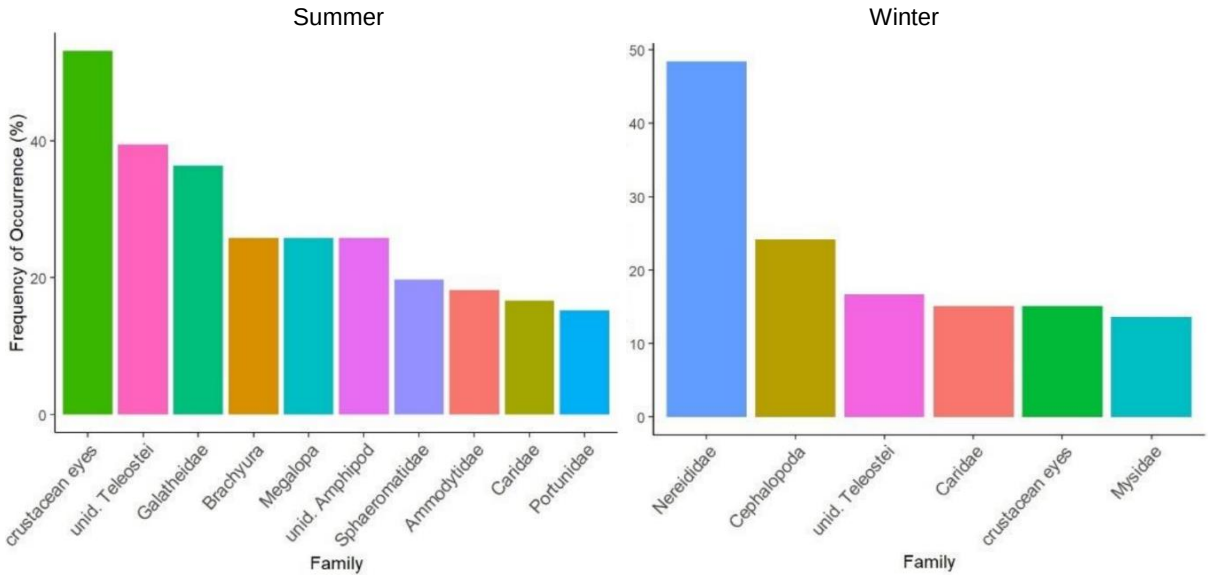

Figure 14. Bar plots showing the prey taxa most frequently present in stomach content samples during summer and winter (expressed as a percentage of the total number of stomachs in each season).

While sex was not a significant factor, the interaction between season and length class significantly influenced prey community composition (pseudo-F = 1.50, $p < 0.05$). This was predominantly driven by the summer sample, which exhibited a clear ontogenetic diet shift from smaller to larger individuals. During this period, small individuals (32–40 cm) primarily consumed juvenile decapods, in particular megalopa larvae and *Galatheidae* spp. Other small decapods, such as juvenile brachyuran crabs and mud shrimp (*Upogebiidae* spp.), were also frequently present, along with amphipods and small teleost fish. Medium-sized individuals (40–58 cm) began consuming larger crustaceans such as *Portunidae* spp. and exhibited higher occurrences of teleosts, including the first recorded presence of sand eels (*Ammodytidae* spp.) in their diet. In contrast, the diet of large pollack (58–66 cm) was dominated by teleosts, with the largest individuals ingesting some particularly sizeable fish prey such as greater sand eels (*Hyperoplus lanceolatus*) and rocklings (Lotidae spp.). Crustacean eyes were frequently observed across all length groups during summer (Figure 15).

In winter, the diet composition was more consistent, with Nereid polychaetes being the first or second most frequently observed prey group across all size classes. Small individuals relied most heavily on *Nereididae* spp., but also consumed amphipods and other crustaceans. In medium-sized individuals, cephalopods and teleosts contributed more substantially to the diet, while in large individuals, *Nereididae* spp. remained dominant, followed by decapod crustaceans and cephalopods. Other crustaceans, such as *Caridea* spp. and *Mysidae* spp., were regularly observed across all size classes during winter (Figure 16).

More detailed results describing the diet composition of Isle of Man pollack are available in Wagner (2025).

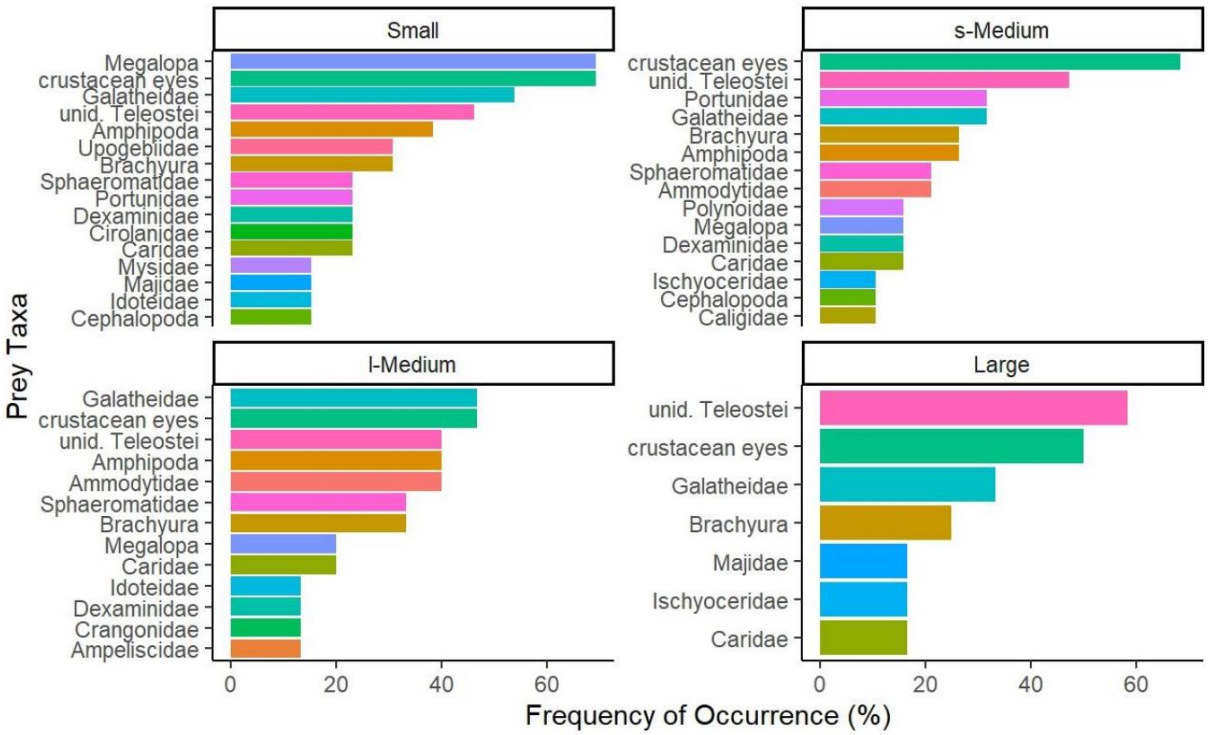

Figure 15. Bar plots showing the prey taxa most frequently present in stomach content samples during summer from different pollack length classes (Small: 32–40 cm; s-Medium: 40–49 cm; l-Medium: 49–58 cm; Large: 58–66 cm).

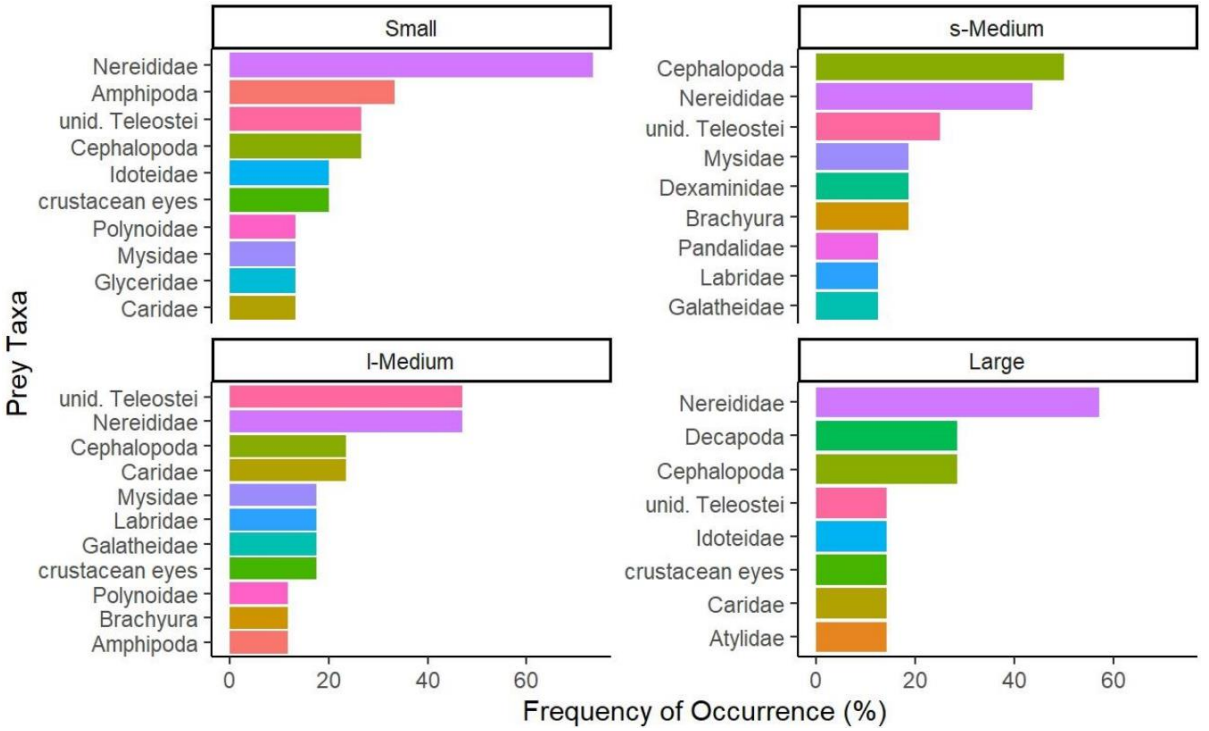

Figure 16. Bar plots showing the prey taxa most frequently present in stomach content samples during winter from different pollack length classes (Small: 32–40 cm; s-Medium: 40–49 cm; l-Medium: 49–58 cm; Large: 58–66 cm).

4. Discussion

This study represents the first comprehensive biological assessment of pollack (*P. pollachius*) in the Isle of Man territorial sea, addressing a crucial knowledge gap for stock management and contributing to the wider body of research underway across the UK following the emergency closure of the fishery. The findings offer novel insights into local stock characteristics and feeding behaviour, and provide a foundation for future monitoring and management efforts.

4.1. Life history and stock status

A variety of key life history parameters encompassing maturity, growth, and mortality were obtained, which underpin stock assessments ranging from data-limited to data-rich approaches. Among these, estimates of size at maturity were derived for the Isle of Man stock during both summer and winter, revealing clear seasonal differences (summer L_{50} = 52.1 cm; winter L_{50} = 43.8 cm). These differences reflect variation in the reproductive state of the population across the year, with the winter estimate considered more reliable due to the presence of enlarged, visibly mature gonads, aligning closely to the pollack spawning period (January–April) (Alonso-Fernández et al., 2013; Stamp et al., 2025; Wilson et al., 2014). In contrast, a smaller proportion of individuals were classified as mature during summer, with the sample consisting of immature and spent/recovering gonad stages.

Notably, the winter L_{50} estimate for Isle of Man pollack (43.8 cm) aligns closely with those obtained elsewhere in the North Atlantic (42–47 cm) (Alemany, 2017; Fischer et al., 2020; Stamp et al., 2025), and is considerably larger than the EU MCRS for the species, set at 30 cm. This highlights a potential depletion of reproductive potential at both local and broader scales. Based on the size-frequency distribution recorded during this study in the Isle of Man, it is estimated ~35% of the landable portion of the catch consists of immature individuals, indicating the stock was likely susceptible to growth overfishing prior to closure. This is further supported by the outputs of the size-based indicators assessment, with those related to the conservation of immatures (L_c and $L_{25\%}$) both classified as being in 'poor' status. Therefore, implementing changes to MCRS regulations prior to reopening the fishery may help conserve the reproductive capacity of the stock and improve long-term sustainability. However, consideration should be given to post-release mortality caused by barotrauma. For instance, descending devices have been shown to mitigate barotrauma-induced mortality in rod-and-line fisheries elsewhere when returning undersized fish. Furthermore, current landing obligations for pollack present legislative barriers to the effectiveness of MCRS increases as a conservation measure, requiring all catches to be landed regardless of size.

In addition to immatures, the growth parameters obtained in this study point to a potential lack of large individuals in the population, which are also important for the reproductive health of the stock and overall resilience to fishing pressure. While L_∞ was estimated at ~90

cm, the largest fish recorded during the sampling period measured 75 cm, with 90% of the catch falling below 60 cm. Concurrently, indicators for the conservation of large individuals ($L_{max5\%}$ and P_{mega}) were both categorised as 'poor' for the Isle of Man stock. However, these results are associated with high uncertainty due to limitations in the underlying growth data, particularly in relation to the estimate of L_∞, which exhibited very wide confidence intervals (95% CI: 71–106 cm). There is also potential for L_∞ to have been overestimated due to the minimal numbers of older age groups (> 6 years) in the sample. Nevertheless, methods were employed in the analysis to reduce this bias, and the values obtained from both approaches (otolith ageing and ELEFAN) are broadly comparable to those reported for the species in other studies (Appendix Table B).

While indicators for the conservation of immature and large individuals may be cause for concern, those related to fishery performance were more positive. Length-based proxies for optimal yield and MSY suggest that the fishery is predominantly catching individuals near the optimum harvest length ($L_{mean}/L_{opt} \approx 1$), and that overall levels of fishing pressure are likely to be sustainable ($L_{mean}/L_{F=M} > 1$). This is further supported by the estimated values obtained for natural mortality (M; 0.31 year^{-1}) and fishing mortality (F; 0.21 year^{-1}), which suggest a moderate exploitation rate (F/M = 0.68). While acknowledging these results were obtained following the closure of the fishery, they remain relevant in understanding selectivity relative to yield optimization and provide an indication of previous exploitation levels – potentially reflecting the historically small scale of the Isle of Man pollack fishery.

In addition to size-based indicators, this study explored the potential use of historic LPUE data in the Isle of Man as an indicator of abundance. Standardised LPUE values, adjusted for seasonal and vessel effects, fluctuated between 4 and 8 kg hour^{-1} from 2000 to 2023, with no clear long-term trend. While this suggests relative stability in catch rates over time, the reliability of hours fished as a proxy for fishing effort in the pollack fishery is unclear, as this metric does not account for gear characteristics (e.g. number of hooks, number of lines). Standardisation for vessel effects (as applied here) may help mitigate these issues by accounting for differences in fishing practices across vessels; however, further research is needed to validate the use of fishing time or identify suitable alternatives. Furthermore, LPUE estimates for the period 2021–2023 are less robust as trip-level fishing times were unavailable, and the absence of data between 2015 and 2020 limits the ability to assess long-term trends. These issues currently constrain the application of catch-based stock assessment methods such as SPiCT (Stochastic Production model in Continuous Time) (Pedersen & Berg, 2017), which rely on consistent and well-defined effort metrics. Therefore, the application of size-based indicators, as demonstrated in this study, may be particularly relevant for the pollack fishery going forward.

4.2. Diet composition

Stomach content analysis undertaken during this study provides useful information for understanding the feeding behaviour of pollack in Isle of Man waters, revealing significant seasonal and ontogenetic variation in diet. Overall, the data suggests the species employs an opportunistic, benthopelagic foraging strategy typical of generalist predators, characterised by high dietary plasticity.

In summer, pollack diets were dominated by juvenile decapod crustaceans, including megalopa larvae and *Galatheidae* spp., which are also key components in the diet of other demersal fishes such as cod, haddock, and whiting (Pinnegar et al., 2003). These prey taxa exhibit strong seasonal pulses in the Irish Sea, with abundances peaking between June and August (Lindley et al., 1994; Öndes et al., 2018; Robinson & Tully, 2000), coinciding with the summer sampling period in this study. Sand eels (*Ammodytidae* spp.) were also frequently consumed during this period, reflecting seasonal recruitment patterns (O'Connell & Fives, 1995). Overall, the variety of prey taxa consumed in summer suggests that pollack feed in both pelagic and benthic environments. Notably, the frequent presence of algal detritus in summer stomach samples (including possible *Laminaria* spp.), along with epifaunal species typically associated with seaweed beds, points to the likely use of structurally complex macroalgal habitats, as previously observed in saithe (*P. virens*) (Sarno et al., 1994).

In contrast, winter stomach content samples contained fewer pelagic prey and were dominated by polychaetes, in particular *Nereididae* spp., which accounted for nearly half of all prey items. Furthermore, the dominant teleost prey groups shifted from sand eels in summer to benthic-associated species such as gobies (*Gobiidae* spp.) and wrasses (*Labridae* spp.) in winter. This pattern suggests increased reliance on benthic habitats during colder months, likely driven by reduced availability of pelagic prey and seasonal changes in habitat use. The preference for nereid polychaetes could be due to a combination of increased accessibility during pre-spawning swarming behaviour (Olive, 1995; Watson et al., 2003) and their nutritional value, containing high levels of lipids and polyunsaturated fatty acids that support gonad development (García-Alonso et al., 2008; Luis & Passos, 1995). Cephalopods, including *Loligo* spp., were also identified as a key prey group in winter, coinciding with their reproductive aggregations in the Irish Sea (Collins et al., 1997; Waluda & Pierce, 1998). This further supports the notion that pollack respond dynamically to seasonal prey availability.

Ontogenetic diet shifts, commonly reported in other demersal gadoids (Day et al., 2019; Jaworski & Ragnarsson, 2006; Mahe et al., 2007), were also observed in this study. As fish increase in size, their energetic requirements rise substantially, driving a shift toward larger, more energy-rich prey such as teleosts (Juanes et al., 2002). This was particularly evident in the summer diet of pollack in Isle of Man waters, with smaller individuals preferring juvenile prey taxa while larger individuals increasingly targeted sand eels and other teleost species. Gape limitations also contribute to this pattern, as smaller fish are physically incapable of handling and ingesting larger prey (Dunic & Baum, 2017; Juanes et al., 2002). Interestingly,

however, this trend was not observed in the winter samples, with all pollack sizes exhibiting a preference for polychaetes and cephalopods as food sources. This suggests energetic demands for reproductive activity during winter may override typical size-based feeding patterns, with these particular prey groups found to offer high energy returns per unit handling time (Fall & Fiksen, 2020).

From a management perspective, the overall dietary plasticity of pollack may buffer short-term fluctuations in prey availability, allowing the species to exploit a variety of prey types across habitats and seasons. However, reliance on ecologically sensitive prey such as nereids, squid, and sand eels, raises potential concerns, as these species are known to be sensitive to climate-driven changes in distribution and recruitment (Heath et al., 2012; Piatkowski et al., 2001). This highlights the importance of considering trophic interactions in fisheries management and stock recovery strategies, especially for a species exhibiting signs of depletion at a broad spatial scale (ICES, 2023).

5. ICES advice for 2026

The 2025 ICES benchmark assessment for pollack (*P. pollachius)* in the Celtic Seas and the English Channel (subareas 6–7) introduces a 'category 1' age-structured stock assessment approach using Stock Synthesis (SS3) (ICES, 2025a). This transition from the previous 'category 2' approach enhances the understanding of stock dynamics by incorporating improved estimates of stock-recruitment relationships and accounting for technological advancements in the fishery that influence catch rates (ICES, 2025b). The new model integrates revised life-history parameters, age-structured commercial landings, length-structured recreational removals, commercial LPUE indices, and a combined scientific survey index. Reference points were also re-estimated (ICES, 2025b).

Current estimates indicate that fishing pressure is below both F_{MSY} and F_{PA}, while spawning-stock biomass remains below MSY $B_{trigger}$ and lies between B_{PA} and B_{lim} (ICES, 2025c). Based on the MSY approach, ICES advises that total removals in 2026 should not exceed 2210 tonnes, encompassing both commercial and recreational catches (accounting for survival of released fish) (ICES, 2025c). This increase from previous zero-catch advice is due to a change in assessment method and the new reference points following the ICES benchmark (ICES, 2025c).

ICES notes that the stock structure of pollack in this ecoregion remains poorly defined, with no conclusive evidence that subareas 6 and 7 represent a distinct biological stock unit (ICES, 2025c). Further research is required to clarify stock identity and, in the interim, the current assessment boundaries have been retained by ICES (ICES, 2025b).

6. Recommendations for Isle of Man fisheries and research

- An increase in the MCRS to align with the L_{50} indicated by winter sampling (~44 cm), with consideration of the implications of landing obligations as well as practices to reduce post-release mortality or improve size selectivity.
- Consideration and/or future research to investigate the benefits of a spawning closure.
- Improved data collection framework for catch and effort data so that a robust LPUE index can be created and used as an input for SPiCT models.
- Quantification of recreational removals due to the recent inclusion in ICES catch advice.
- Continuation of a self-sampling framework to obtain length-frequency data from commercial catches and monitor length-based indicators.

7. References

Alemany, J. (2017). Développement d'un cadre Bayésien pour l'évaluation de stocks à données limitées et élaboration de scénarios de gestion, cas particuliers de la seiche (Sepia officinalis) et du lieu jaune (Pollachius pollachius). *University of Caen Normandy PhD Thesis*, 238 pp.

Alonso-Fernández, A., Villegas-Ríos, D., Valdés-López, M., Olveira-Domínguez, B., & Saborido-Rey, F. (2013). Reproductive biology of pollack (Pollachius pollachius) from the Galician shelf (north-west Spain). *Journal of the Marine Biological Association of the United Kingdom*, *93*(7), 1951–1963. https://doi.org/10.1017/S0025315413000283

Bucholtz, R. H., Tomkiewicz, J., Dalskov, J., Wilhelms, I., Sell, A., Bland, B., Vitale, F., Gibb, I., & Power, G. (2007). Manual to determine gonadal maturity of North Sea saithe (Pollachius virens L). *National Institute of Aquatic Resources, Department of Marine Fisheries, Technical University of Denmark*, 29 pp.

Collins, M. A., Pierce, G. J., & Boyle, P. R. (1997). Population indices of reproduction and recruitment in Loligo forbesi (Cephalopoda: Loliginidae) in Scottish and Irish waters. *Source: Journal of Applied Ecology*, *34*(3), 778–786.

Day, L., Kopp, D., Robert, M., & Le Bris, H. (2019). Trophic ecology of large gadiforms in the food web of a continental shelf ecosystem. *Progress in Oceanography*, *175*, 105–114. https://doi.org/10.1016/j.pocean.2019.03.007

DEFRA. (2024). Report of the 1st EU-UK Expert Workshop on Pollack. *Specialised Committee on Fisheries, 18 April 2024*, 24pp.

Dunic, J. C., & Baum, J. K. (2017). Size structuring and allometric scaling relationships in coral reef fishes. *Journal of Animal Ecology*, *86*(3), 577–589. https://doi.org/10.1111/1365-2656.12637

Fall, J., & Fiksen, Ø. (2020). No room for dessert: A mechanistic model of prey selection in gut-limited predatory fish. *Fish and Fisheries*, *21*(1), 63–79. https://doi.org/10.1111/faf.12415

Fischer, S. H., de Oliveira, J. A. A., & Kell, L. T. (2020). Linking the performance of a data-limited empirical catch rule to life-history traits. *ICES Journal of Marine Science*, *77*(5), 1914–1926. https://doi.org/10.1093/icesjms/fsaa054

García-Alonso, J., Müller, C. T., & Hardege, J. D. (2008). Influence of food regimes and seasonality on fatty acid composition in the ragworm. *Aquatic Biology*, *4*(1), 7–13. https://doi.org/10.3354/ab00090

Heath, M. R., Neat, F. C., Pinnegar, J. K., Reid, D. G., Sims, D. W., & Wright, P. J. (2012). Review of climate change impacts on marine fish and shellfish around the UK and Ireland. *Aquatic Conservation: Marine and Freshwater Ecosystems*, *22*(3), 337–367. https://doi.org/10.1002/aqc.2244

Heino, M., Svsand, T., Nordeide, J. T., & Otter, H. (2012). Seasonal dynamics of growth and mortality suggest contrasting population structure and ecology for cod, pollack, and

saithe in a Norwegian fjord. *ICES Journal of Marine Science*, *69*(4), 537–546. https://doi.org/10.1093/icesjms/fss043

ICES. (2012). Stock Annex: Pollack (Pollachius pollachius) in Subarea 8 and Division 9.a (Bay of Biscay and Atlantic Iberian waters). *Working Group for the Bay of Biscay and the Iberic Waters Ecoregion (WGBIE)*, 4 pp.

ICES. (2018). ICES reference points for stocks in categories 3 and 4. *ICES Technical Guidelines*, 50 pp. https://doi.org/10.17895/ices.pub.4128

ICES. (2023). Pollack (Pollachius pollachius) in subareas 6-7 (Celtic Seas and the English Channel). *ICES Advice on Fishing Opportunities, Catch and Effort, Pol.27.67*, 8 pp. https://doi.org/10.17895/ices.advice.21841011

ICES. (2025a). Benchmark workshop on the application of Stock Synthesis (SS3) on selected stocks (WKBSS3). ICES Scientific Reports. 7:25. 191 pp. https://doi.org/10.17895/ices.pub.28443992

ICES. (2025b). Working Group for the Celtic Seas Ecoregion (WGCSE). ICES Scientific Reports. 7:52. 957 pp. https://doi.org/10.17895/ices.pub29401877

ICES. (2025c). Pollack (Pollachius pollachius) in subareas 6-7 (Celtic Seas and the English Channel). *ICES Advice on Fishing Opportunities, Catch and Effort, Pol.27.67*, 8 pp. https://doi.org/10.17895/ices.advice.27202803

Jaworski, A., & Ragnarsson, S. Á. (2006). Feeding habits of demersal fish in Icelandic waters: a multivariate approach. *ICES Journal of Marine Science*, *63*(9), 1682–1694. https://doi.org/10.1016/j.icesjms.2006.07.003

Juanes, F., Buckel, J. A., & Scharf, F. S. (2002). Feeding Ecology of Piscivorous Fishes. In *Handbook of Fish Biology and Fisheries* (Vol. 1, pp. 267–283). Blackwell Publishing Ltd.

Lindley, J. A., Williams, R., & Conway, D. V. R. (1994). Variability in dry weight and vertical distributions of decapod larvae in the Irish Sea and North Sea during the spring. *Marine Biology*, *120*, 385–395.

Luis, O. J., & Passos, A. M. (1995). Seasonal changes in lipid content and composition of the polychaete Nereis (Hediste) diversicolor. *Comparative Biochemistry and Physiology Part B: Biochemistry and Molecular Biology*, *111*(4), 579–586.

Mahe, K., Amara, R., Bryckaert, T., Kacher, M., & Brylinski, J. M. (2007). Ontogenetic and spatial variation in the diet of hake (Merluccius merluccius) in the Bay of Biscay and the Celtic Sea. *ICES Journal of Marine Science*, *64*(6), 1210–1219. https://doi.org/https://doi.org/10.1093/icesjms/fsm100

O'Connell, M., & Fives, J. M. (1995). The Biology of the Lesser Sand-Eel Ammodytes tobianus L. In the Galway Bay Area. *Biology and Environment: Proceedings of the Royal Irish Academy*, *95*(2), 87–98.

Olive, P. J. W. (1995). Annual breeding cycles in marine invertebrates and environmental temperature: Probing the proximate and ultimate causes or reproductive synchrony. *Journal of Thermal Biology*, *20*(1–2), 79–90.

Öndes, F., Kaiser, M. J., & Murray, L. G. (2018). Fish and invertebrate by-catch in the crab pot fishery in the Isle of Man, Irish Sea. *Journal of the Marine Biological Association of the United Kingdom*, *98*(8), 2099–2111. https://doi.org/10.1017/S0025315417001643

Pedersen, M. W., & Berg, C. W. (2017). A stochastic surplus production model in continuous time. *Fish and Fisheries*, *18*(2), 226–243. https://doi.org/10.1111/faf.12174

Piatkowski, U., Pierce, G. J., & Morais Da Cunha, M. (2001). Impact of cephalopods in the food chain and their interaction with the environment and fisheries: An overview. *Fisheries Research*, *52*(1–2), 5–10. https://doi.org/https://doi.org/10.1016/S0165-7836(01)00226-0

Pinnegar, J. K., Trenkel, V. M., Tidd, A. N., Dawson, W. A., & Du Buit, D. M. H. (2003). Does diet in Celtic Sea fishes reflect prey availability? *Journal of Fish Biology*, *63*, 197–212. https://doi.org/10.1046/j.1095-8649.2003.00204.x

Robinson, M., & Tully, O. (2000). Seasonal variation in community structure and recruitment of benthic decapods in a sub-tidal cobble habitat. *Marine Ecology Progress Series*, *206*, 181–191.

Sarno, B., Glass, C. W., & Smith, G. W. (1994). Differences in diet and behaviour of sympatric saithe and pollack in a Scottish sea loch. *Journal of Fish Biology*, *45*, 1–11. https://doi.org/10.1111/j.1095-8649.1994.tb01080.x

Stamp, T., Stewart, B. D., Thomas, S., Uren, D., Mawer, R., Nesbit, R., Davies, P., Hall, A., Osmond, T., Conlon, R., Rudd, H., Hyder, K., Roberts, J., & Sheehan, E. V. (2025). *Pollack Fisheries Industry Science Partnership (FISP): Project Outputs*. 46 pp.

Then, A. Y., Hoenig, J. M., Hall, N. G., & Hewitt, D. A. (2015). Evaluating the predictive performance of empirical estimators of natural mortality rate using information on over 200 fish species. *ICES Journal of Marine Science*, *72*(1), 82–92. https://doi.org/10.1093/icesjms/fsu136

Wagner, F. (2025). Investigating the diet of data-limited Pollachius pollachius to inform future fisheries management. *Bangor University MSci Thesis*, 47 pp.

Waluda, C. M., & Pierce, G. J. (1998). Temporal and spatial patterns in the distribution of squid Loligo spp. In United Kingdom waters. *African Journal of Marine Science*, *20*, 323–336.

Watson, G. J., Bentley, M. G., Gaudron, S. M., & Hardege, J. D. (2003). The role of chemical signals in the spawning induction of polychaete worms and other marine invertebrates. *Journal of Experimental Marine Biology and Ecology*, *294*(2), 169–187. https://doi.org/10.1016/S0022-0981(03)00264-8

Wilson, L. J., Burrows, M. T., Hastie, G. D., & Wilson, B. (2014). Temporal variation and characterization of grunt sounds produced by Atlantic cod Gadus morhua and pollack Pollachius pollachius during the spawning season. *Journal of Fish Biology*, *84*(4), 1014–1030. https://doi.org/10.1111/jfb.12342

8. Appendix

Table A. Visual maturity staging criteria used in this study, taken from the guide developed by ICES for saithe (P. virens) (Bucholtz et al., 2007).

Stage	**1**		**2**		**3**			**4**	**5**
Definition	**Juvenile/immature**		**Maturing**		**Spawning**			**Spent**	**Resting**
	Early	Preparation	Early	Late	Initiation	Main period	Cessation		
Maturity classification	**Immature**		**Mature**					**Mature (spent/recovering)**	
Female visual description	Small, elongated ovaries; posterior in body cavity; translucent purple-reddish.	Small, but easily distinguishable ovaries; posterior in body cavity; smooth surface; slightly translucent.	Ovaries still small and posterior in body cavity; firmer than Stage 1; slightly uneven surface; opaque orange.	Ovaries reached maximum size; firm with prominent blood vessels; opaque orange/light pink; oocytes clearly visible and densely packed.	Ovaries extending length of body cavity; distended and soft; opaque orange/light pink; single, glassy oocytes among abundant opaque oocytes; lumen may contain fluid or glassy oocytes.	Ovaries fill most of body cavity; very distended and soft; granulated orange/light pink; mixture of glassy and opaque oocytes; lumen containing excess fluid or glassy oocytes.	Flabby, shrunken ovaries; glassy oocytes present with few or no opaque oocytes; lumen containing excess fluid and abundant glassy oocytes.	Contracted, slack ovaries; greyish cast; translucent dark purple-red; opaque oocytes absent but single, glassy oocytes may occur.	Ovaries small, similar to Stage 1 (preparation); slightly uneven surface; translucent purple-red with greyish cast.
Male visual description	Small, string-like testes; posterior in body cavity; tiny, glassy lobules; transparent or translucent red.	Small, but easily distinguishable testes; posterior in body cavity; small, blurred lobules; translucent red.	Testes still small and posterior in body cavity; soft, plump lobules; blood vessels visible; opaque red.	Testes enlarged; dorsal in body cavity; brittle, plump lobules; empty, transparent spermatoducts with prominent blood vessels; opaque reddish-white.	Testes extending into ventral part of body cavity; brittle, distended lobules; spermatoducts filled with viscous fluid; opaque creamy white.	Testes large and prominent in body cavity; soft, plump lobules; spermatoducts filled with milky fluid; opaque whitish.	Soft, flabby testes; shrunken to dorsal part of body cavity; lobules almost empty; spermatoducts still containing fluid; opaque reddish-purple.	Testes contracted and flabby; posterior in body cavity; lobules empty; spermatoducts with signs of previous distension; red with greyish cast.	Testes small, similar to Stage 1 (preparation); spermatoducts visible; red with greyish cast.

Table B. Previous values for the asymptotic length (L_∞) of pollack (P. pollachius) stocks reported in the literature.

Location	L_∞ **(cm)**	**Reference**
Bay of Biscay and Iberian Coast	85.6	ICES (2012)
English Channel	88.6–90.4	Stamp et al. (2025)
ICES Subareas 6–7	98.2	Alemany (2017)
North Wales	97.3	Stamp et al. (2025) using data from 1989
Norway	62.0	Heino et al. (2012)